

## Supplementary Information for

### Molecular Dynamics and Kinetics of Isothermal Cold Crystallization

#### with Tunable Dimensionality in a Molecular Glass Former,

#### 5'-(2,3-Difluorophenyl)-2'-ethoxy-4-pentyloxy-2,3-difluorotolane

Tomasz Rozwadowski,<sup>1,2</sup> Hiroshi Noda,<sup>1</sup> Łukasz Kolek,<sup>3</sup> Mizuki Ito,<sup>1</sup> Yasuhisa Yamamura,<sup>1</sup>

Hideki Saitoh,<sup>4</sup> and Kazuya Saito<sup>1</sup>

<sup>1</sup>Department of Chemistry, Faculty of Pure and Applied Sciences, University of Tsukuba,

Tsukuba, Ibaraki 305-8571, Japan

<sup>2</sup>Department of Chemical and Process Engineering, Faculty of Chemistry,

Rzeszow University of Technology, 35-959 Rzeszow, Poland

<sup>3</sup>Department of Material Science, Faculty of Mechanical Engineering and Aeronautics,

Rzeszow University of Technology, 35-959 Rzeszow, Poland

<sup>4</sup>Graduate School of Science and Engineering, Saitama University,

Saitama 338-8570, Japan

S.I Crystal Structure of CrI Phase of DFP25DFTP

S.II Differential Scanning Calorimetric Analysis of Phase Behavior of DFP25DFTP

S.III Standard Thermodynamic Quantities for Stable Phases (Liquid & CrI Phase) of DFP25DFTP

S.IV Relative Molecular Energy for a Torsion Angle of Selected Rotatable Bonds

## S.I Crystal Structure of Cr1 phase of DFP25DFT

Crystallographic data as a CIF file have been deposited with Cambridge Crystallographic Data Centre under the registry CCDC 2164890. The structure is illustrated in Fig. S1.

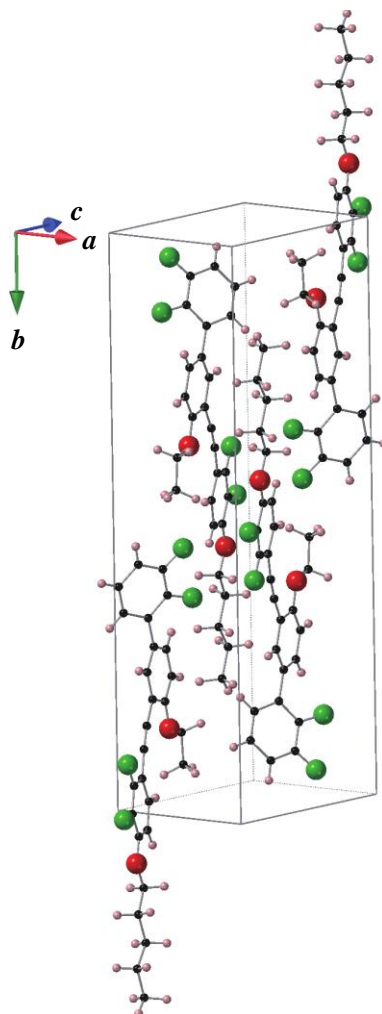


Figure S1. Crystal structure of Cr1 phase of DFP25DFT at room temperature.

## S.II Differential Scanning Calorimetric Analysis of Phase Behavior of DFP25DFT

A commercial differential scanning calorimeter (TA Instruments Q200) was used to establish the phase behavior. Before use, a standard calibration procedure using indium and zinc standards for temperature and energy was applied. Both the as-supplied powder and recrystallized single-crystals from ethanol were subject to analyses.

The analyses always started from room temperature to 183 K, then turned into heating to 370 K, and cooling to room temperature. We conducted them while keeping the temperature ramp rate ( $\pm 1$ ,  $\pm 5$ , or  $\pm 10$  K  $\text{min}^{-1}$ ) during a series of experiments for each sample. Since the initial crystalline state was not recovered by thermal treatment once melted, we used fresh specimens for each series of measurements. Note that we could refresh the thermal memory of the sample by melting. The behavior after melting was mostly reproduced irrespective of different thermal histories.

The as-supplied specimen (Cr1 phase) did not exhibit anomaly in the initial cooling, melted at 340 K on heating, and vitrified (changed to the liquid-quenched glass) around 250 K during successive cooling, irrespective of the temperature ramp rate (Figs. S2, S3 & S4). When the heating was fast ( $\pm 10$  K  $\text{min}^{-1}$ ), no significant anomaly was detected except for the glass transition (Fig. S4). The heating of the glass at a slow or medium rate induced crystallization in a broad temperature range (depending on the rate) after softening around 250 K of the glass (Figs. S2 & S3). Cold-crystallized samples exhibit complicated traces. Essentially, it exhibits melting around 324 K through a transient crystalline phase, Cr2', while accompanying the crystallization to another crystal Cr3, which melts at 335 K. Annealing at room temperature of the sample cold-crystallized around 300 K yields neat phase Cr2. The cold-crystallization at temperature higher than 324 K yielded the phase Cr3 with a melting temperature of 335 K.

The single-crystals melted at the same temperature as the as-supplied specimen, indicating the same phase state. Accordingly, the successive behavior coincided with the as-supplied specimen.

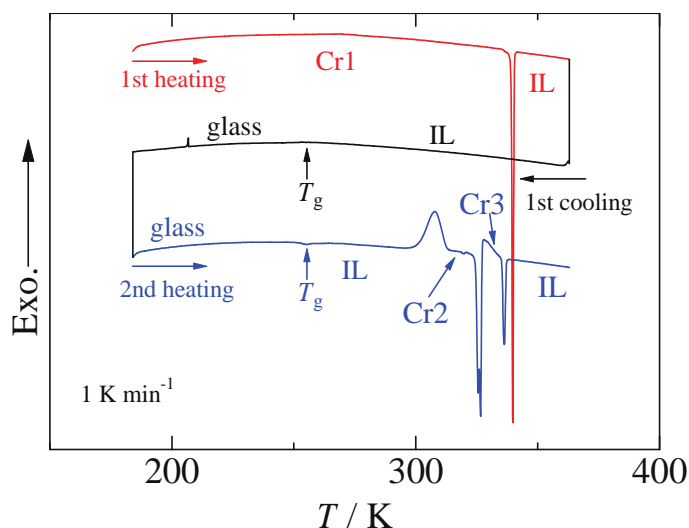


Figure S2. DSC trace of the as-supplied DFP25DFT at the temperature ramp rate of 1 K  $\text{min}^{-1}$ .

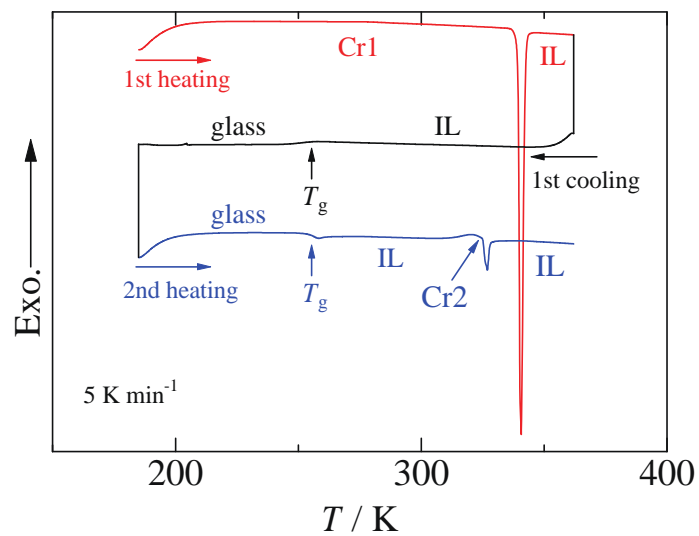


Figure S3. DSC trace of the as-supplied DFP25DFT at the temperature ramp rate of 5 K min<sup>-1</sup>.

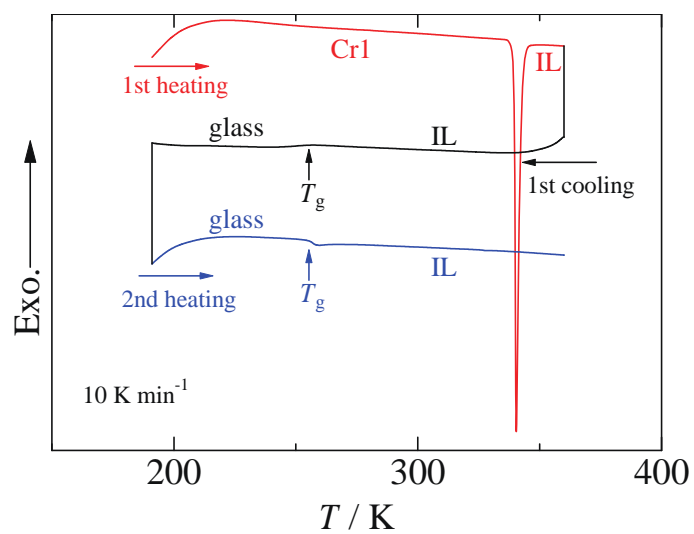


Figure S4. DSC trace of the as-supplied DFP25DFT at the temperature ramp rate of 10 K min<sup>-1</sup>.

S.III Standard Thermodynamic Quantities for Stable Phases (Liquid & CrI Phase) of DFP25DFT

Table S1. Standard thermodynamic functions of crystalline DFP25DFT at round temperature  $T$ .  $C_p$ , molar isobaric heat capacity;  $H(T)$ , molar enthalpy;  $S(T)$ , molar entropy;  $G(T)$ , molar Gibbs energy.

$\frac{T}{\text{K}}$	$\frac{C_p^\circ}{\text{J K}^{-1} \text{ mol}^{-1}}$	$\frac{[H^\circ(T) - H^\circ(0)]/T}{\text{J K}^{-1} \text{ mol}^{-1}}$	$\frac{S^\circ(T) - S^\circ(0)}{\text{J K}^{-1} \text{ mol}^{-1}}$	$\frac{-[G^\circ(T) - H^\circ(0)]/T}{\text{J K}^{-1} \text{ mol}^{-1}}$
CrI phase				
10	11.24	3.15	4.18	1.02
20	39.13	13.96	20.23	6.28
30	68.99	27.36	41.78	14.43
40	97.13	41.32	65.53	24.21
50	123.47	55.15	90.06	34.92
60	148.12	68.61	114.78	46.17
70	171.18	81.64	139.37	57.73
80	192.79	94.19	163.65	69.46
90	213.21	106.29	187.55	81.25
100	232.71	117.97	211.03	93.06
110	251.56	129.26	234.09	104.84
120	269.88	140.22	256.77	116.55
130	287.77	150.88	279.08	128.20
140	305.31	161.29	301.05	139.76
150	322.59	171.47	322.71	151.24
160	339.70	181.45	344.07	162.63
170	356.74	191.26	365.18	173.92
180	373.78	200.92	386.05	185.13
190	390.88	210.47	406.72	196.25
200	408.10	219.92	427.20	207.28
210	425.47	229.29	447.54	218.24
220	443.03	238.61	467.73	229.12
230	460.83	247.88	487.82	239.93
240	478.91	257.13	507.81	250.68
250	497.32	266.37	527.73	261.36

260	516.09	275.61	547.60	271.99
270	535.27	284.87	567.44	282.57
280	554.90	294.16	587.26	293.09
290	575.03	303.50	607.08	303.58
300	595.70	312.89	626.92	314.03
310	616.94	322.36	646.80	324.44
320	638.81	331.90	666.73	334.83
330	661.35	341.54	686.73	345.19
340.0	683.90	351.28	706.81	355.53
Fusion				
Liquid phase				
340.0	804.69	460.46	815.99	355.53
350	814.54	470.44	839.46	369.02
360	824.06	480.13	862.54	382.41
370	833.17	489.55	885.24	395.69
298.15	591.83	311.15	623.25	312.10

#### S.IV Relative Molecular Energy for a Torsion Angle of Selected Rotatable Bonds

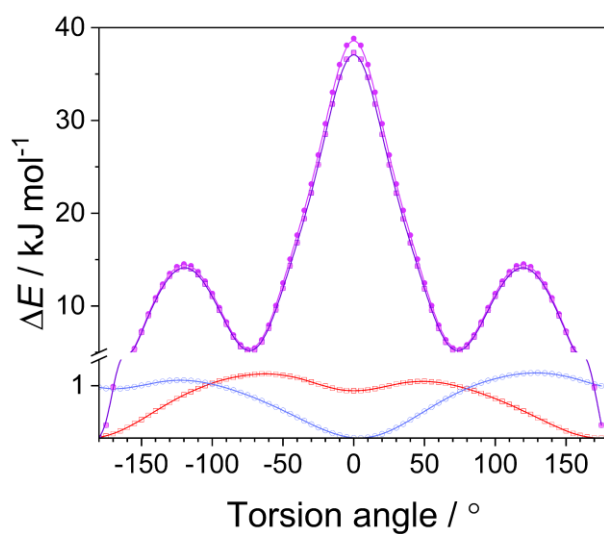


Figure S5. Relative molecular energy  $\Delta E$  for a torsion angle of selected bonds.